International Journal of Multiphase Flow 155 (2022) 104172

Contents lists available at ScienceDirect

International Journal of Multiphase Flow

journal homepage: www.elsevier.com/locate/ijmulflow

A mechanistic model for the prediction of flow pattern transitions during separation of liquid-liquid pipe flows

Nikola Evripidou [a], Carlos Avila [b], Panagiota Angeli [a,*]

[a] ThAMeS Multiphase, Department of Chemical Engineering, University College London, London WC1E 7JE, United Kingdom
[b] Avila Multiphase Flow Consulting, 27410 Guthrie Ridge Ln, Katy, TX 77494, USA

ARTICLE INFO

Keywords:
Two-phase flow
Dispersion
Oil-water
Separation
Mechanistic model

ABSTRACT

A one-dimensional mechanistic model that predicts the flow pattern transitions during the separation of dispersed liquid-liquid flows in horizontal pipes was developed. The model is able to capture the evolution along the pipe of the four characteristic layers that develop from initially dispersed flows of either oil-in-water or water-in-oil at a range of mixture velocities: a pure water layer at the bottom, a settling (flotation/sedimentation) layer, a dense-packed zone, and a pure oil layer on the top. Coalescence correlations from literature were included in the model to predict the drop growth due to binary drop coalescence and the coalescence rate of drops with their corresponding interface. The model predictions on the evolution of the heights of the different layers were partly compared against available experimental data obtained in a pilot scale two-phase flow facility in a test section of 0.037 m inner diameter using tap water and an oil of density 828 kg m^{-3} and viscosity 5.5 mPa s as test fluids, and in a 0.1 m inner diameter test section using water and an oil of density 857 kg m^{-3} and viscosity 13.6 mPa s. It was shown that the evolution of the four characteristic layers depends on the rates of drop settling and drop-interface coalescence. Oil-in-water dispersions separated faster than water-in-oil ones, while dispersions with smaller drop-sizes were more likely to exhibit depletion of the dense-packed zone.

1. Introduction

Pipe flows of two immiscible liquids are common in the engineering sector and are often encountered in chemical and nuclear plants, and in the oil and gas industry (Danielson 2012). Dispersions can be formed as part of the process or in equipment such as choke valves and bends. These dispersions may be unstable and separate further downstream. The tendency to separate can be exploited to design in-line separators, which are often favourable to other separators as they are simple, small, and lightweight with low operating cost (Zhong et al., 2013). In the oil and gas industry, they can be employed to increase oil recovery, hence have the potential to extend the operational lifetime of older oil fields by making extraction economically viable (Skjefstad and Stanko, 2019). On the other hand, in cases where dispersions are important for enhancing mass transfer, minimising pipe erosion (Wang and Zhang, 2016) or frictional losses during transportation of crude oil (Pilehvari et al., 1988), the tendency of liquid-liquid mixtures to separate can be detrimental.

Unstable dispersions of two immiscible liquids can undergo gravity-controlled separation while flowing through horizontal pipes (Perez, 2005; Voulgaropoulos and Angeli, 2017). Separation is always observed, unless the dispersions are stabilised by surfactants or by flow-induced mixing at high flow velocities. The separation process is rather complex and depends on several factors including the properties of the fluids, the size distribution of the drops present, the mixture velocity, and the pipe diameter and inclination.

Several authors have studied the separation of dispersions experimentally and in different set-ups, including batch and steady-state settlers, and pipe flows. Ryon et al. (1960) was the first to experimentally investigate the separation of liquid-liquid dispersions, while Barnea and Mizrahi (1975) noted the existence of a dense-packed zone. Later, Hartland and Jeelani (1988) explained the batch separation in terms of the physical processes occurring. According to them, dispersions in batch and steady-state settlers consist of settling and dense-packed layers. The drops grow in size due to drop-drop coalescence in the settling layer, they accumulate into a dense-packed zone near the liquid-liquid interface, and finally coalesce with their homophase. They also noted that the rate of settling depends on the drop size and hold-up of the dispersed phase, while the interfacial coalescence rate is a function of the drop size at the coalescing interface and the thickness of the

* Corresponding author.
E-mail address: p.angeli@ucl.ac.uk (P. Angeli).

https://doi.org/10.1016/j.ijmultiphaseflow.2022.104172
Received 16 November 2021; Received in revised form 10 June 2022; Accepted 23 June 2022
Available online 25 June 2022

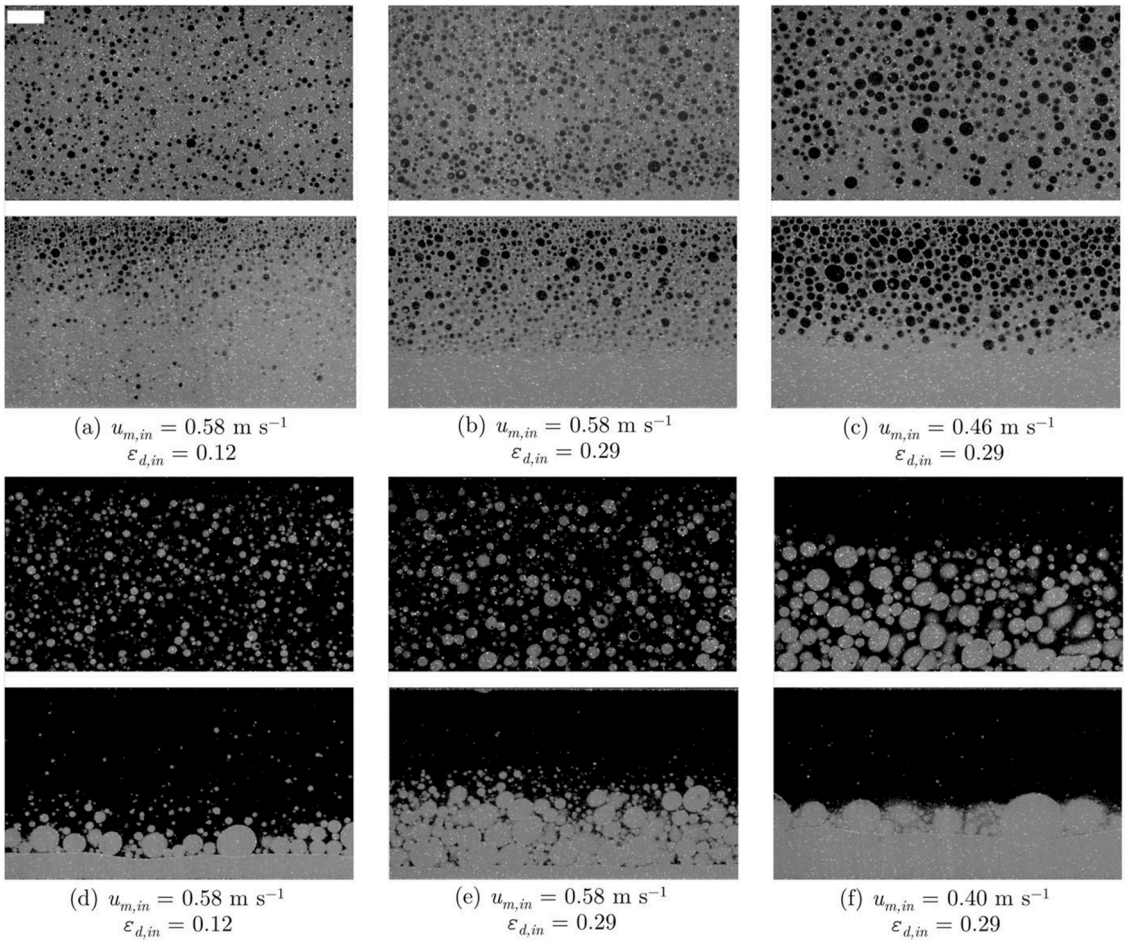

Fig. 1. Planar Laser-Induced Fluorescence images acquired for a few typical flow conditions investigated downstream of the static mixer at x^+=15 (top) and x^+=135 (bottom). The scale bar is 5 mm long. (a)–(c) correspond to cases of water-continuous dispersions, while (d)–(f) to correspond to cases of oil-continuous.(Voulgaropoulos et al., 2019)[1]

dense-packed layer. More recent works studied the separation of dispersed flows in horizontal pipes. Pérez (2005) and Voulgaropoulos et al. (2019) used a static mixer to generate dispersions which were then fed to a horizontal pipe and observed significant stratification downstream of the inlet at low mixture velocities (cf. Fig. 1). Conan et al. (2007) and Voulgaropoulos et al. (2016) employed different multi-nozzle inlet configurations to generate dispersions at low velocities and reported similar findings to those shown in Fig. 1.

From experiments, it was concluded that the separation of dispersions in pipes is driven by three main mechanisms: 1) drop settling (i.e. flotation or sedimentation), 2) drop-drop coalescence, and 3) drop-interface coalescence. Assuming a fully dispersed oil-in-water flow in a horizontal pipe, separation would begin as the lower density oil drops begin to float upwards. This results in the formation of a pure water layer at the bottom of the pipe. As the drops continue to float, the thickness of the pure water layer increases. Eventually, some drops reach the top of the pipe where they accumulate into a dense-packed zone. Within the dense-packed zone, the drops come into contact with each other for long enough for coalescence to occur. This process continues and eventually a thin film of pure oil forms at the top of the pipe. Coalescence of drops with the liquid film results in an increase in the thickness of the pure oil layer. This process continues until complete separation is achieved.

As the dispersions settle and layers form along the pipe, different flow patterns emerge. Accurate characterization of the flow pattern transitions in unstable dispersed flows is vital for the design and operation of industrial facilities. In the last decades, there has been a significant increase on research focused on the flow of liquid-liquid mixtures, however work on flow pattern transitions remains limited. The information available, is often limited to measurements of the phase holdup and the pressure gradient of the mixtures (Oddie and Pearson, 2004), as the opaque fluids or test sections and the difficult thermodynamic conditions restrict the implementation of several sampling techniques. Usually, laboratory experiments are implementing model oils to observe and identify different flow configurations at steady state (Trallero et al., 1997; Angeli and Hewitt, 2000; Elseth, 2001; Simmons and Azzopardi, 2001; Lovick and Angeli, 2004; Voulgaropoulos and Angeli, 2017; Voulgaropoulos et al., 2019). Computational fluid dynamics (CFD) approaches have also been used as they can provide phase distribution with high resolution. Thus far, few CFD studies have been reported on predicting the flow pattern and phase distribution in horizontal oil-water flows (Walvekar et al, 2009; El-Batsh, 2012; Pouraria et al., 2016, Voulgaropoulos et al. 2019). The prediction of the flow patterns and the phase fraction profiles at low mixture velocities where the effect of gravity becomes significant and transitions take place is even more complex. Accurate models for the prediction of the flow pattern evolution and the separation length in dispersions can provide

[1] Reproduced from Voulgaropoulos, V, Jamshidi, R, Mazzei, L, Angeli, P (2019). "Experimental and numerical studies on the flow characteristics and separation properties of dispersed liquid-liquid flows". In: *Physics of Fluids* 31.7, p. 073304., with the permission of AIP Publishing. doi: https://doi.org/10.1063/1.5092720

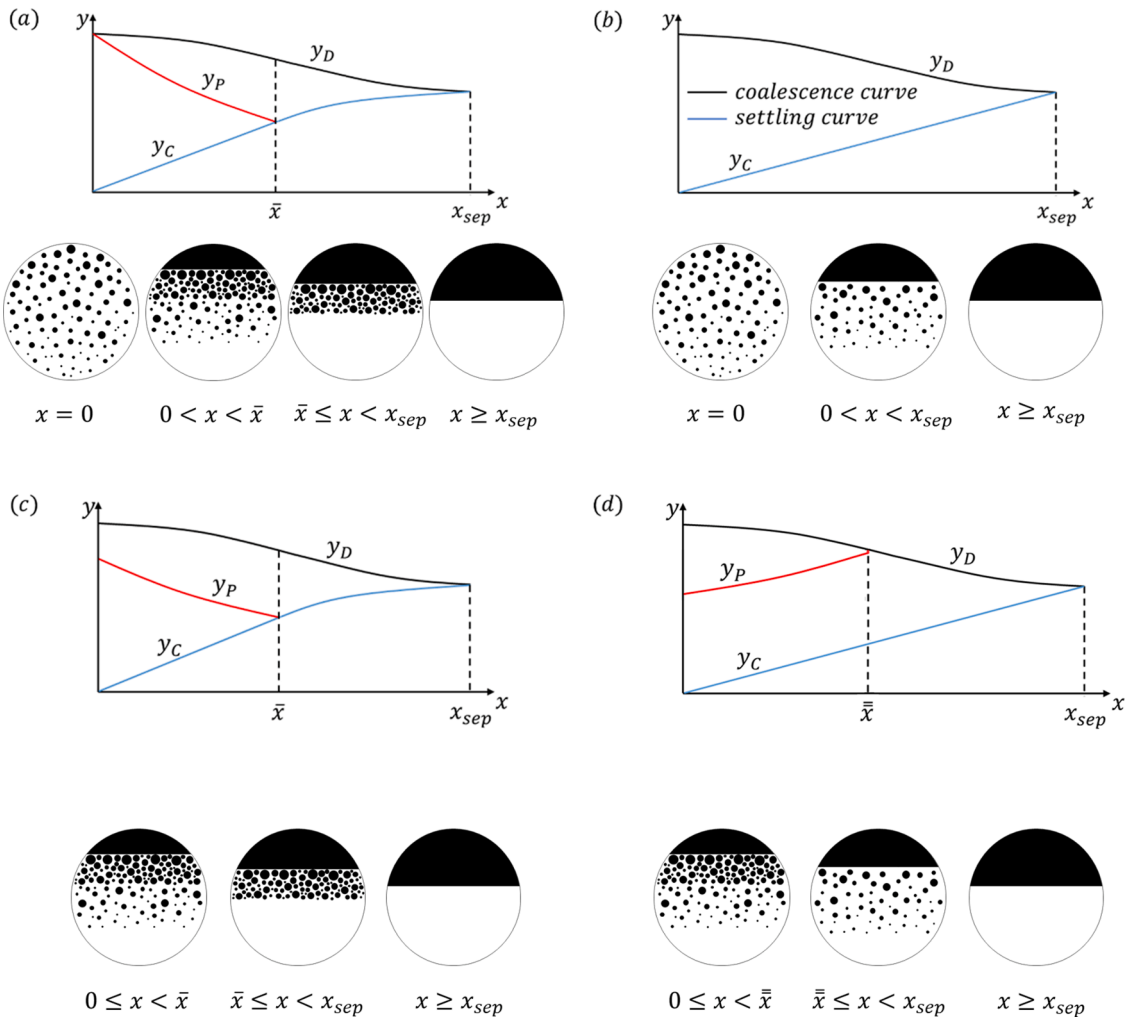

Fig. 2. Schematics of flow profiles showing the evolution of the characteristic layers and the flow patterns along the pipe for dispersed liquid-liquid systems with different inlet conditions.

information for systems where experimental data is sparse.

Previously a few authors attempted to model the separation of dispersions in batch settlers using simplified mechanistic models (Hartland and Jeelani, 1988; Jeelani and Hartland, 1998; Henschke et al, 2002). Later works attempted to extend the batch models to one-dimensional flows in horizontal pipe separators (Pereyra et al., 2013; Othman et al., 2018) by changing the time scale to a length scale using the average mixture velocity and accounting for the change in geometry. Mechanistic models can be an attractive alternative to complex CFD simulations due to their low computational time. Nevertheless, current mechanistic models on separation of dispersions in pipe flows assume that the rate of drop settling is larger than the coalescence rate, hence accumulation of drops into a dense-packed zone is predicted at the liquid-liquid interface. Although this is always true in batch vessels, this is not always the case in pipe flows (Voulgaropoulos, 2017; Evripidou et al., 2019). In dispersed pipe flows of relatively high mixture velocities and small drop diameters the drop settling rate may be similar or even lower than the rate of coalescence and a dense-packed layer may not form. Consequently, current mechanistic models are only valid for certain flow configurations and flow pattern transitions, and cannot be applied to all pipe flows.

In this work, we develop a universal mechanistic model that can predict the flow pattern development and separation of unstable liquid-liquid dispersed pipe flows. New approaches are proposed to predict all possible flow pattern transitions occurring during flow separation, which are not captured in existing models. The model is based on the horizontal pipe separator approach described in Pereyra et al. (2013), which is valid only for systems where a dense-packed layer is formed. In what follows, we identify all flow pattern transitions during separation of dispersions. We then describe the development of the model, placing emphasis on the pipe locations where only a dilute dispersed layer is present, which is often the case in systems of high mixture velocities or small drops, and which are not predicted by previous mechanistic models. Lastly, we demonstrate the applicability of the model to flows of both oil-in-water and water-in-oil dispersions. The model accounts for the main mechanisms that occur during pipe flow and can be used to provide information on the evolution of dispersed flows in systems where sampling is not feasible.

2. Mechanistic modelling

The separation of liquid-liquid dispersions is driven by three main mechanisms: drop settling (flotation or sedimentation), drop-drop coalescence, and drop-interface coalescence. Separation can give rise to four distinct layers: a pure layer of the continuous phase, a settling layer (a dilute dispersion where drop settling occurs), a dense-packed layer (a densely packed dispersion where drop-drop coalescence occurs), and a pure layer of the initially dispersed phase. Throughout this paper, the four layers are denoted by the subscripts C, S, P, and D respectively.

Fig. 2 shows schematics of different flow profiles that can arise from

fully or partially dispersed flows at the pipe inlet and the flow patterns observed along the pipe in each case. The flow profiles are plots that show the progression of the characteristic layers along the pipe. On the x-axis, they have the axial displacement from the pipe inlet and on the y-axis the height from the bottom of the pipe. The *settling (flotation/sedimentation) curve* is given by y_C, and in an oil-in-water dispersion, it corresponds to the height of the water layer from the bottom of the pipe. The *coalescence curve*, denoted by y_D, gives the location of the pure oil interface. The *dense-packed zone curve, y_P*, gives the interface between the settling and dense-packed layers. The thickness, h, of each of the characteristic layers is dependent on drop settling rate, as well as the drop-drop and drop-interface coalescence rates. If the rate of drop settling is faster than the rate of drop-interface coalescence, accumulation of drops into a dense-packed zone is observed at the oil-water interface (cf. Fig. 2(a)). Within the dense-packed zone, the drops are in close proximity and the contact time often exceeds the coalescence time leading to drop-drop coalescence and an increase in the average drop size along the pipe. Coalescence of the oil drops with the bulk oil phase also occurs and results in an increase of the oil layer thickness with pipe length. Depletion of the settling layer is possible as the flow evolves, as shown in Figs. 2(a) and 2(c) at $x = \bar{x}$. Alternatively, if the rate of drop settling is smaller than the rate of drop-interface coalescence, the dense-packed zone is depleted. This is the case in Fig. 2(d) at $x = \bar{\bar{x}}$. At lengths greater than $\bar{\bar{x}}$ (i.e. for $x > \bar{\bar{x}}$), the settling layer is in direct contact with the pure oil layer and the rate of drop settling (and availability of drops at the interface) limits the rate of coalescence. If the flow is initially fully dispersed, but the drop settling rate is less than the drop-interface coalescence rate, the rate of drop settling will control the rate of coalescence throughout the pipe, and a dense-packed zone will never form (cf. Fig. 2(b)). The length required to reach complete separation of the two immiscible liquids ($x = x_{sep}$) can be determined from the intersection point of the *coalescence curve* and the *settling curve*.

The mechanistic model developed here predicts the changes in thickness of the various layers and the mean drop diameter along the pipe, giving the complete flow profile up to the point of complete phase separation. The model assumes a constant velocity, equal to the mixture velocity u_M, across all layers along the spanwise direction, thus neglecting velocity profiles and exchange of momentum between the layers. This is a reasonable assumption for liquid-liquid systems where experiments showed that the slip is very small, especially in the dispersed regions (Rodriguez and Oliemans, 2004; Lovick and Angeli, 2004). The surface tension is assumed to be constant throughout, while the mixture is assumed to be monodispersed. Drop break-up is not considered. Although in reality there is no apparent interface between the two dispersed layers, settling and dense-packed (cf. Fig. 1), for modelling purposes, it was assumed that these are two distinct layers. The dispersed-phase fraction within each layer is taken as constant with height and a step-change in the fraction is assumed at the interface between the two layers.

Below the various parts of the model are described in detail.

2.1. Settling curve

The primary separation mechanism acting on a dispersed liquid-liquid mixture is density-driven settling. In the presence of a settling layer, the *settling curve*, y_C, changes solely due to the vertical displacement of drops. In an oil-in-water dispersion, the *settling curve* corresponds to the height of the pure water layer from the bottom of the pipe and can be predicted in terms of pure water layer thickness, h_C, by

$$\frac{dh_c}{dx} = \frac{u_s}{u_M}. \tag{1}$$

Assuming a continuous phase of viscosity μ_C and density ρ_C, and a dispersed phase of viscosity μ_D and density ρ_D, the vertical (sedimentation/flotation) velocity u_s of drops of size d_p, within a settling layer with dispersed-phase fraction φ_S can be obtained using

$$u_s = C_h \frac{3\lambda\varphi_S\mu_C}{C_w\xi(1-\varphi_S)\rho_C d_p}\left[\left(1 + Ar\frac{C_w\xi(1-\varphi_S)^3}{54\lambda^2\varphi_S^2}\right)^{0.5} - 1\right]. \tag{2}$$

Eq. (2) is based on an empirical model developed by Pilhofer and Mewes (1979) from drop settling experiments in batch vessels, but has been modified by Evripidou et al. (2019) who introduced a fitted hindered settling parameter, C_h, to better capture delay in settling due to the flow. This correlation was developed for a monodispersed system taking as the average drop diameter the Sauter mean diameter in the settling layer. In Eq. (2) the two settling parameters are equal to

$$\lambda = \frac{1-\varphi_S}{2\varphi_S K_{HR}}\exp\left(\frac{2.5\varphi_S}{1-0.61\varphi_S}\right) \tag{3}$$

and

$$\xi = 5K_{HR}^{-\frac{3}{2}}\left(\frac{\varphi_S}{1-\varphi_S}\right)^{0.45}. \tag{4}$$

Other dimensionless numbers include the Archimedes number, Ar, which is given by

$$Ar = \frac{\rho_C\Delta\rho g d_p^3}{\mu_C^2} \tag{5}$$

where g is the gravitational constant, the Hadamard-Rybczynski factor, K_{HR}, given by

$$K_{HR} = \frac{3(\mu_C + \mu_D)}{2\mu_C + 3\mu_D}, \tag{6}$$

and a modified friction coefficient, C_W, given by

$$C_w = \frac{Ar}{6Re_\infty^2} - \frac{3}{K_{HR}Re_\infty}. \tag{7}$$

The Re_∞ is the Reynolds number of a single drop moving vertically in an infinite medium. According to Ishii and Zuber (1979)

$$Re_\infty = 9.72\left[(1 + 0.01Ar)^{\frac{4}{7}} - 1\right]. \tag{8}$$

In the absence of a settling layer (i.e. for $x > \bar{x}$ in Figs. 2(a) and 2(c)), the thickness of the continuous phase layer can be obtained by

$$h_C = ID - h_P - h_D, \tag{9}$$

where ID denotes the internal diameter of the pipe.

2.2. Coalescence curve

Accumulation of drops near the top of the pipe due to drop settling results in coalescence. Eventually a continuous oil layer of thickness h_D is formed. The increase in h_D with pipe length is captured by the *coalescence curve*, y_D, and is determined by the volume rate of coalescence of drops with the oil interface. Assuming a monodispersed mixture at the interface, where all drops have the same diameter $d_{p,I}$, Pereyra (2011) showed that the evolution of the oil layer thickness along a horizontal pipe is given by

$$\frac{dh_D}{dx} = \frac{2\varphi_I d_{p,I}}{3\tau_I u_M}, \tag{10}$$

where τ_I is the drop-interface coalescence time. In the presence of a dense-packed layer, we set the oil fraction at the interface, φ_I, to 0.9 which is a reasonable value for maximum packing for a polydispersed mixture (Farr and Groot, 2009; Dorr et al., 2013). In the absence of a dense-packed layer (i.e. Fig. 2(b) and Fig. 2(d) for $x > \bar{\bar{x}}$), such that the

settling layer is in direct contact with the pure oil layer, we suggest that φ_I is determined by the relative rates of drop settling and drop-interface coalescence. Assuming monodispersed layers, the average drop diameter at the interface $d_{p,I}$ is taken to be equal to the Sauter mean diameter in the respective dispersed layer (dense-packed or settling).

2.3. Drop size evolution

Drop-drop coalescence can only occur if the contact time between two drops exceeds the drop-drop coalescence time, τ_C. The relative motion of the drops with respect to each other is negligible within the dense-packed layer and along the coalescing interface, thus drop-drop coalescence is always considered in these locations. Following the assumption that all layers are monodispersed, at every axial location the drops found along the interface or within a dense-packed layer, have the same size $d_{p,I}$. Hartland and Jeelani (1998) suggested the following expression for the prediction of drop size evolution as a function of drop-drop coalescence time τ_C:

$$\frac{d(d_{p,I})}{dx} = \frac{d_{p,I}}{6\tau_C u_M}. \tag{11}$$

To estimate the coalescence rate within the more dilute settling layer, we computed the Reynolds numbers for the case studies considered here. We found that the settling layer falls into the transition to turbulent flow regime. Thus, we estimated the coalescence rates, by modifying the correlations suggested in Coulaloglou and Tavlarides (1977) to apply to pipe flows. The drop-drop coalescence rates were found to be insignificant, hence drop-drop coalescence within the settling layer is not considered further in this work.

2.4. Coalescence time

Of the few correlations available in literature for the calculation of coalescence rates or times (Jeelani and Hartland, 1994; Henschke et al., 2002), the one suggested by Henschke et al. (2002) was incorporated in the model, as presented in Pereyra et al. (2013). Henschke et al. (2002) assumed film drainage during coalescence and concluded that the drop-drop and drop-interface coalescence times can be obtained by

$$\tau_C = \frac{(6\pi)^{7/6}\mu_C r_a^{7/3}}{4\sigma^{5/6}H^{1/6}r_{F,C}r_V^*} \tag{12}$$

and

$$\tau_I = \frac{(6\pi)^{7/6}\mu_C r_a^{7/3}}{4\sigma^{5/6}H^{1/6}r_{F,I}r_V^*} \tag{13}$$

respectively. In Eqs. (12) and (13), σ is the interfacial tension between the two phases. r_V^* is the asymmetry parameter describing the asymmetry of the film between adjacent drops. It can be obtained from experimental settling curves and is characteristic for the system used. The Hamaker coefficient H is set to 10^{-20} N m, as proposed by Henschke et al. (2002) for any system. The drop-drop contact area radius $r_{F,C}$ is calculated by

$$r_{F,C} = 0.3025 d_p \sqrt{1 - \frac{4.7}{La + 4.7}}, \tag{14}$$

the drop-interface contact area radius $r_{F,I}$ can be related to the drop-drop contact area radius using equation

$$r_{F,I} = \sqrt{3} r_{F,C} \tag{15}$$

and the radius of the channel contour formed when three drops approach, r_a, is given by

$$r_a = 0.5 d_p \left(1 - \sqrt{1 - \frac{4.7}{La + 4.7}}\right). \tag{16}$$

La is a modified Laplace number and is given by

$$La = \left(\frac{|\rho_C - \rho_D|g}{\sigma}\right)^{0.6} \widetilde{h}_P{}^{0.2} d_p. \tag{17}$$

La accounts for the close packing of drops and represents the ratio between the hydrostatic pressure and the interfacial tension. The hydrostatic pressure is a result of the drop-packing height below the draining film, $\widetilde{h}_P$. Consequently, $\widetilde{h}_P$ equals to the thickness of the dense-packed zone if one is present. In the absence of a dense-packed zone, the settling layer is in direct contact with the pure oil layer. In that case, we suggest that $\widetilde{h}_P$ is taken to be equal to the drop size at the interface $d_{p,I}$.

2.5. Settling layer dispersed-phase fraction

In initially fully dispersed flows, the dispersed-phase volume fraction of the settling layer φ_S is equal to the oil volume fraction at the inlet, φ_0. However, in cases where the flow is partially separated at the inlet, such as the cases shown in Figs. 2(c) and 2(d), φ_S can differ to φ_0. In that instance, φ_S can be obtained from a mass balance on the pipe cross section

$$\varphi_S = \frac{A_{pipe}\varphi_0 - A_{D,0} - A_{P,0}\varphi_{P,0}}{A_{S,0}}, \tag{18}$$

where A is the cross-sectional area, while the subscript 0 denotes quantities at the pipe inlet.

2.6. Dense-packed layer thickness and dispersed-phase fraction

Assuming that all four characteristic layers are present at a given axial location from the inlet, we calculate the change in the thickness of the dense-packed layer by performing a mass balance on the pipe cross-sectional area. The cross-sectional area of the dense-packed layer is given by

$$A_P = \frac{A_{pipe}(\varphi_0 - \varphi_S) - A_D(1 - \varphi_S) + A_C\varphi_S}{\varphi_P - \varphi_S} \tag{19}$$

where φ_P is the average dispersed-phase fraction in the dense-packed layer. In the presence of a settling layer the average hold-up of the dense-packed layer is taken equal to

$$\varphi_P = \frac{\varphi_S + \varphi_I}{2} \tag{20}$$

as suggested by Henschke et al. (2002). In Eq. (20) $\varphi_I = 0.9$. If depletion of the settling layer occurs, Eq. (19) simplifies to

$$A_P = \frac{A_{pipe}\varphi_0 - A_D}{\overline{\varphi}_P}. \tag{21}$$

In this case, the average holdup in the dense-packed zone is given by $\overline{\varphi}_P$. In the absence of a settling layer, we allowed $\overline{\varphi}_P$ to increase from its previous value. According to Henschke et al. (2002), since the *settling curve* is continuous at $x = \bar{x}$ (cf. Figs. 2(a) and 2(c)), the holdup φ_P in the region $x \geq \bar{x}$ can be calculated by the following exponentially increasing expression:

$$\overline{\varphi}_P = \varphi_I - \exp\left(-C_1\frac{x}{u_M} - C_2\right). \tag{22}$$

C_1 and C_2 are coefficients determined based on continuity ensuring that at $x = \bar{x}$, $\varphi_P = \overline{\varphi}_P|_{\bar{x}}$. The two coefficients are given by

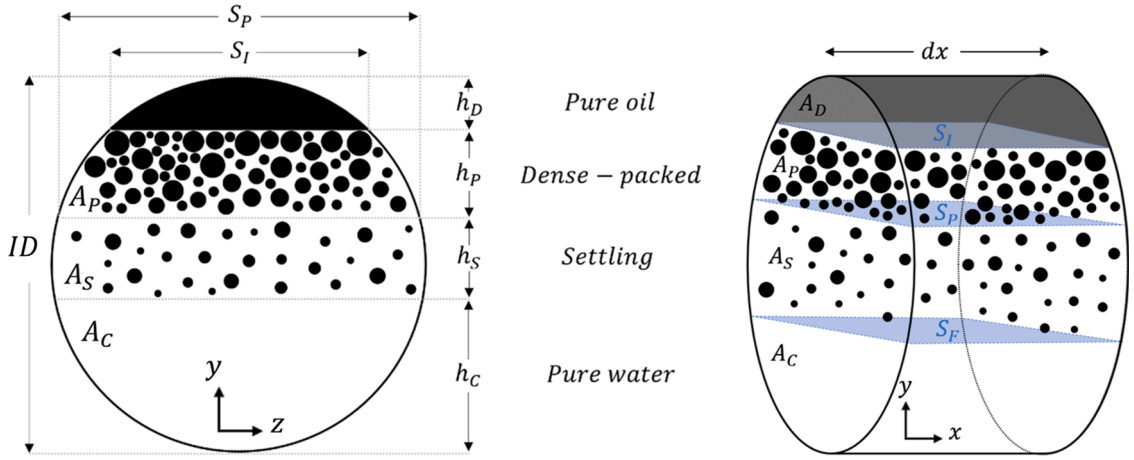

Fig. 3. Schematic of a pipe with oil-in-water dispersed flow.

$$C_1 = \frac{\overline{\varphi}_P|_{\bar{x}}^2 \psi}{(A_{pipe}\varphi_0 - A_D)(\varphi_I - \overline{\varphi}_P|_{\bar{x}})} \quad (23)$$

and

$$C_2 = -C_1\frac{\bar{x}}{u_M} - \ln(\varphi_I - \overline{\varphi}_P|_{\bar{x}}), \quad (24)$$

where, according to Pereyra et al. (2013),

$$\psi = \left[\frac{\partial A_P}{\partial h_P}\left(u_s + u_M\frac{dh_D}{dx}\right) - \frac{u_M}{\overline{\varphi}_P|_{\bar{x}}}\frac{\partial A_D}{\partial h_D}\frac{\partial h_D}{\partial x} - u_M\frac{\partial A_P}{\partial h_D}\frac{\partial h_D}{\partial x}\right]_{x=\bar{x}} \quad (25)$$

If at any axial location, the calculated thickness of the dense-packed layer is smaller than the estimated drop size within the layer (i.e. if $h_P < d_p$), we suggest that depletion of the dense-packed layer occurs and Eq. (19) reduces to

$$A_P = 0. \quad (26)$$

This transition is shown at the location $x = \bar{\bar{x}}$ in Fig. 2(d). At that point, the settling layer comes into contact with the pure oil layer and the dense-packed layer is replaced by a monolayer of drops.

2.7. Settling layer/Oil layer interface

The oil fraction at the coalescing interface φ_I, is very high in the presence of a dense-packed layer. In this paper, we set that to 0.9. In the absence of the dense-packed layer, where the settling layer is in direct contact with the pure oil layer, φ_I is determined by the relative rates of settling and drop-interface coalescence and can be estimate by

$$\varphi_I = \frac{A_{pipe}\varphi_0 - A_D - A_S\varphi_S}{A_I}. \quad (27)$$

In this case, if φ_I reaches the average hold-up of the dense-packed layer φ_P as calculated in Eq. (20), we expect a dense-packed layer to form.

If the dense-packed layer does not form, once the thickness of the settling layer becomes smaller than the drop diameter, the oil fraction at the interface is the same as the oil fraction remaining in the dispersion

$$\varphi_I = \frac{A_{pipe}\varphi_0 - A_D}{A_S}. \quad (28)$$

2.8. Geometric equations

The cross-sectional area of the pure continuous water phase, as shown in Fig. 3, is given by

$$A_C = \frac{ID^2}{4}\left[\pi - \cos^{-1}(\omega_C) + (\omega_C)\sqrt{1-\omega_C^2}\right], \quad (29)$$

where $\omega_C = \frac{2h_C}{ID} - 1$.

The area of the pure oil layer is

$$A_D = \frac{ID^2}{4}\left[\pi - \cos^{-1}(\omega_D) + (\omega_D)\sqrt{1-\omega_D^2}\right], \quad (30)$$

where $\omega_D = \frac{2h_D}{ID} - 1$, and its partial derivative is

$$\frac{\partial A_D}{\partial h_D} = 2\sqrt{h_D(ID - h_D)}. \quad (31)$$

The area of the dense-packed zone can be calculated from

$$A_P = \frac{ID^2}{4}\left[\pi - \cos^{-1}(\omega_P) + (\omega_P)\sqrt{1-\omega_P^2}\right] - A_D, \quad (32)$$

where $\omega_P = \frac{2(h_P+h_D)}{ID} - 1$, and its partial derivative by

$$\frac{\partial A_P}{\partial h_P} = 2\sqrt{(h_D + h_P)(ID - h_P - h_D)}. \quad (33)$$

$\frac{\partial A_P}{\partial h_D}$ can be obtained from the difference of $\frac{\partial A_P}{\partial h_P}$ and $\frac{\partial A_D}{\partial h_D}$, as

$$\frac{\partial A_P}{\partial h_D} = \frac{\partial A_P}{\partial h_P} - \frac{\partial A_D}{\partial h_D} = 2\sqrt{(h_D + h_P)(ID - h_P - h_D)} - 2\sqrt{h_D(ID - h_D)}. \quad (34)$$

The area of the monolayer of drops along the coalescing interface can be calculated from

$$A_I = \frac{ID^2}{4}\left[\pi - \cos^{-1}(\omega_I) + (\omega_I)\sqrt{1-\omega_I^2}\right] - A_D, \quad (35)$$

where $\omega_I = \frac{2(d_{p1}+h_D)}{ID} - 1$.

Finally, a mass balance on the cross-section gives the area of the settling layer as

$$A_S = ID - A_D - A_C - A_P. \quad (36)$$

3. Model implementation

The equations presented above were solved numerically using gPROMS ModelBuilder along the pipe length at steps of 0.1 m. The input parameters required for the model include the fluid properties (densities, viscosities, and surface tension) and the pipe diameter. The drop size at the inlet and the initial thickness of each layer are also needed to

Table 1
Inlet conditions of the experiments.

u_M (m s^{-1})	φ_0
0.52	0.30
	0.45
1.04	0.15
	0.30
	0.45
	0.60

initialize the simulation.

The conditions at which transitions between flow patterns occur can be specified to allow the code to transition between sets of equations. For an initial oil-in-water dispersed flow, the conditions for each transition were specified as follows:

Dense-packed layer formation (cf. Fig. 2(a)). If a uniform settling layer is present at the pipe inlet, a dense-packed layer is assumed to form if the oil interface becomes concentrated. We assume that this occurs once $\varphi_I = \varphi_P$.

Depletion of the settling layer (cf. $x = \bar{x}$ in Figs. 2(a) and 2(c)), i.e. transition from stratified mixed flow with dispersed settling and dense-packed layers to stratified mixed flow with a dispersed dense-packed layer only occurs when the *settling curve* y_C meets the *dense-packed zone curve* y_P (i.e. if $y_C = y_P$). Since the equations in gPROMS were solved at discrete lengths along the pipe, if at any step the *settling curve* is calculated to be higher than the dense-packed layer interface (i.e. if $y_C > y_P$), depletion of the settling layer is assumed.

Depletion of the dense-packed layer (cf. $x = \bar{\bar{x}}$ in Fig. 2(d)), i.e. transition from stratified mixed flow with dispersed settling and dense-packed layers to stratified mixed flow with a dispersed settling layer is assumed to occur if the thickness of the dense-packed layer becomes smaller than the average drop diameter in the layer (i.e. $d_p > h_P$).

Transition to fully stratified flow (cf. $x = x_{sep}$ in Fig.2) occurs when the *settling curve* y_C meets the *coalescence curve* y_D. Hence, if at any step the *settling curve* is found higher than the *coalescence curve* (i.e. if $y_C > y_D$) stratification has been achieved.

4. Results

The experimental data used to assess the performance of the mechanistic model were obtained in a two-phase liquid-liquid flow facility discussed in detail in Voulgaropoulos et al. (2016). In the experiments, tap water and oil (828 kg m^{-3}, 5.5 mPa s, 0.029 N m^{-1}) were used as test fluids. The test section was a transparent acrylic pipe with an internal diameter of 37 mm and overall length of around 8 m. Partial dispersions of oil in water were generated at the inlet of the test section using a multi-nozzle mixer. High-speed imaging was employed at three locations along the spanwise dimension of the pipe to enable the identification of the flow patterns. A dual-conductance probe was implemented to measure the local volume fractions and the drop size distributions of the mixture along a vertical pipe diameter. Measurements were taken every 2 mm, spanning the whole pipe diameter. The equations presented in the paper were solved for six cases with different inlet conditions shown in Table 1.

The hindered settling parameter C_h was taken to be equal to 0.01 as proposed by Voulgaropoulos (2017), while the asymmetric dimple parameter r_V^* was taken to be equal to 0.007, a value that was obtained experimentally by Pereyra et al. (2013) for a similar system. The predicted nondimensionalized flow profiles are presented in Figs. 4 and 5 together with experimental measurements to allow comparison. Nondimensionalization of the layer heights and the pipe length was performed using the internal diameter of the pipe. Dimensionless quantities are denoted with $^+$.

At the low mixture velocity, the drops initially float towards the top of the pipe causing the height of the water layer y_C^+, to increase linearly as expected by Eq. (1). Meanwhile, the height of the dense-packed layer y_P^+ decreases until it meets the *settling curve*. At this pipe length, the settling process is complete and all drops are found within the dense-packed layer. Coalescence between drops within the dense-packed layer results in an increase in the average drop diameter at the interface. Coalescence between the drops and the oil-water interface causes the oil layer to increase in thickness (interface decreases in height). Eventually complete separation occurs as the oil layer curve meets the water layer one. Little difference is observed in the length of complete separation between the two different oil fractions flowing at 0.52 m s^{-1}. No correlation between the separation length and the oil fraction can be established, as the total separation length is dependent on several variables, including the mixture velocity, the thickness of the dispersed layer at the inlet, and the drop size.

At the high mixture velocity of 1.04 m s^{-1} the inlet is almost fully dispersed. In cases (a)-(c) in Fig. 5 the dispersed layer consists of a single settling layer only, while both the dense-packed and the settling layers

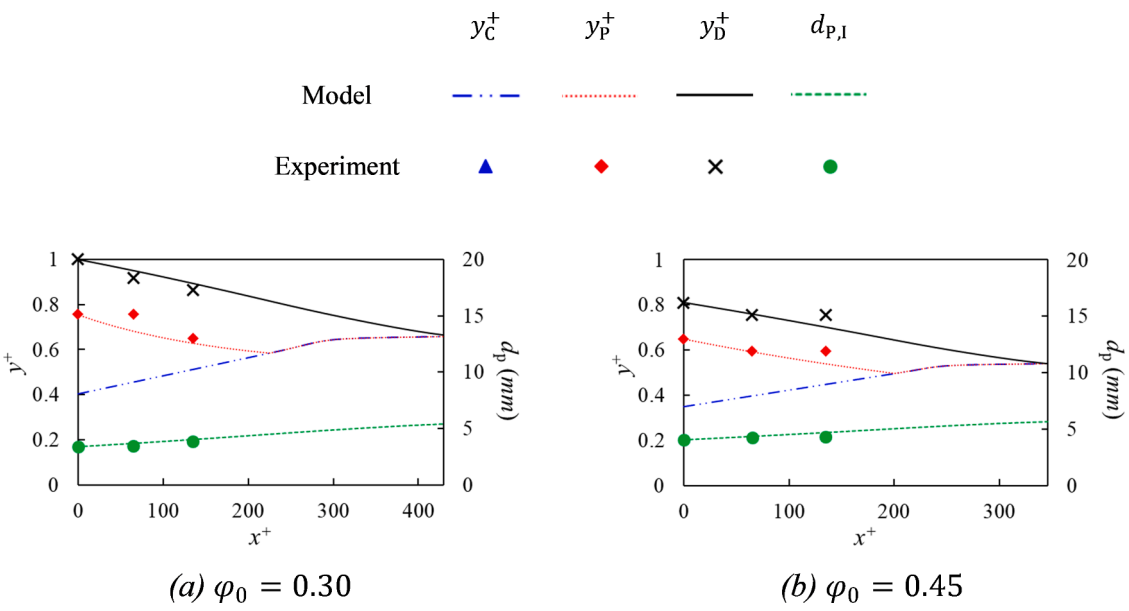

Fig. 4. Predictions of the flow profile and the Sauter mean diameter for oil-in-water dispersions flowing at $u_M = 0.52$ m s^{-1}.

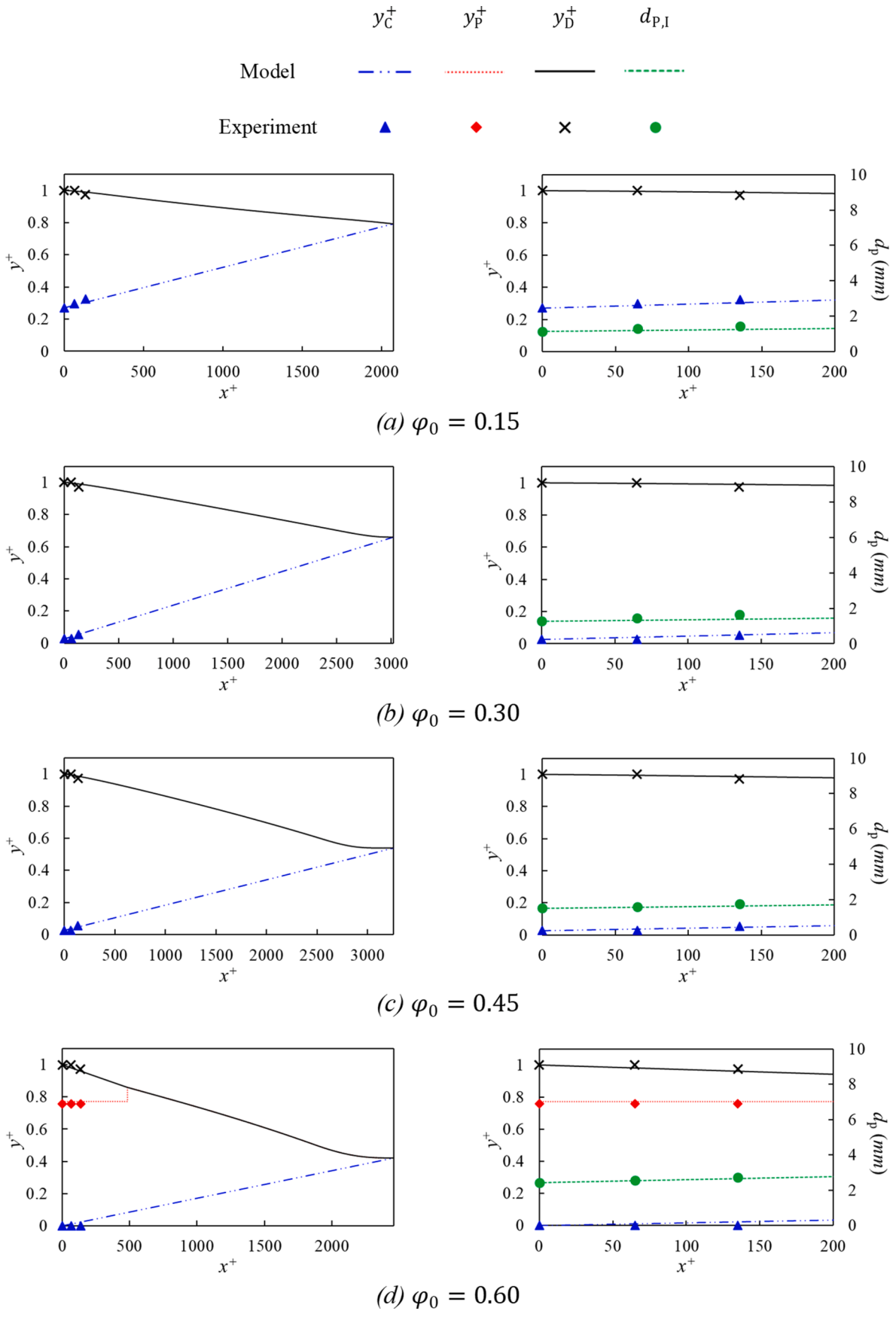

Fig. 5. Predictions of the flow profile and the Sauter mean diameter for oil-in-water dispersions flowing at $u_M = 1.04$ m s^{-1}.

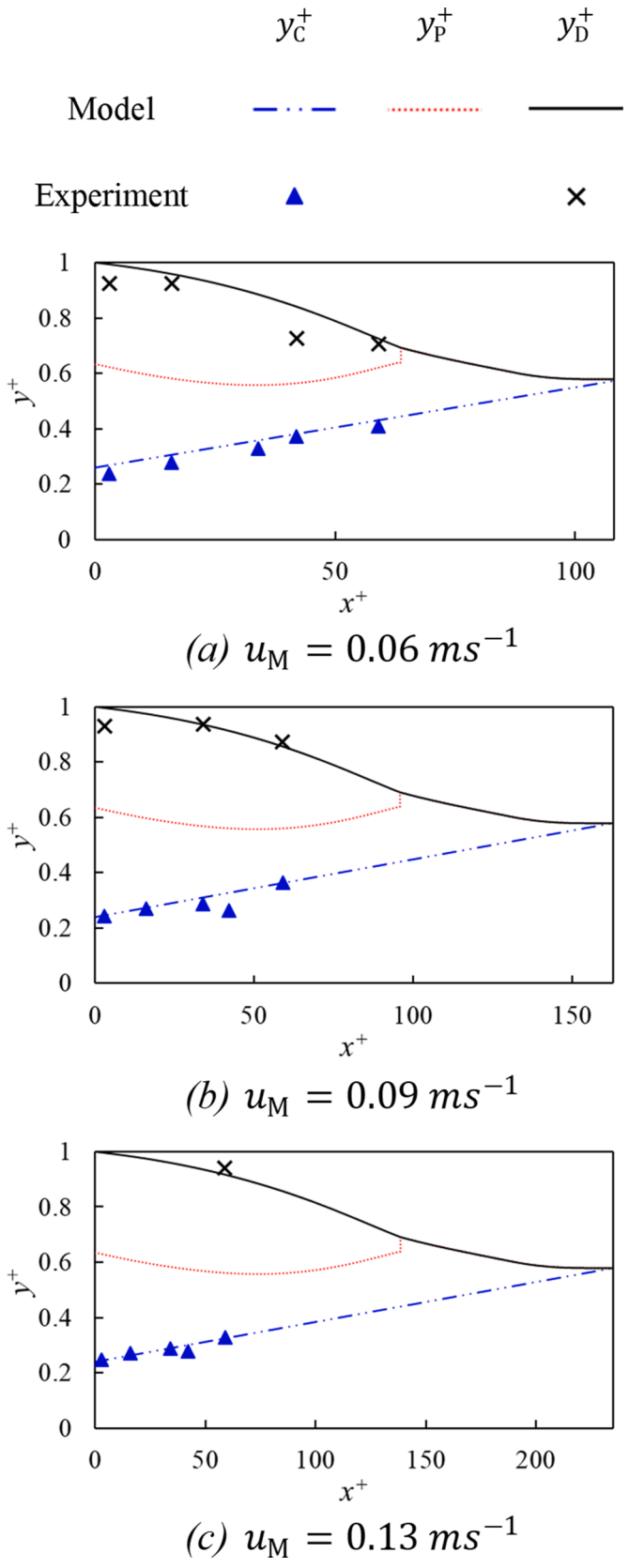

Fig. 6. Predictions of the flow profiles for oil-in-water dispersions with $\varphi_0 = 0.40$ and comparison with experimental data obtained by Pereyra et al. (2013).

are present in case (d). At this velocity, the initial dispersions consist of smaller drops than those present at the low mixture velocity. This results in a smaller settling velocity as shown by the smaller gradient of the *settling curve*; hence, the water layer height increases at a lower rate. In cases (a)-(c), the low settling rate limits the rate of separation, and a dense-packed layer does not form. In case (d) the rate of drop-interface coalescence is faster than the settling rate. This causes the dense-packed layer to decrease in thickness, until it eventually completely depletes and the settling layer comes in direct contact with the pure oil layer. Settling and coalescence continue in a similar fashion until complete separation occurs. Longer separation lengths are predicted at $u_M = 1.04\ m\ s^{-1}$ as settling is the controlling separation mechanism.

The results show that liquid-liquid mixtures at different flow conditions may approach separation in a different manner. These differences result from the relative rates of drop settling and drop-interface coalescence. A higher rate of settling than that of drop-interface coalescence results in the depletion of the settling layer, as seen in the flow profiles of the lower mixture velocity in Fig. 4. On the contrary, higher rates of drop-interface coalescence than those of settling may cause the dense-packed layer to deplete if present at the inlet and the settling layer to persist up to the point of complete separation. This shift in the controlling mechanism is not a result of the change in the mixture velocity itself, but rather a consequence of the smaller drops generated at the inlet as a result of the higher mixture velocity.

The suggested model was also validated against experimental data from Pereyra et al. (2013) to assess its ability to predict the *settling curve*. The experimental data were obtained in a horizontal pipe separator of 0.1 *m* inner diameter and 6 *m* length, using tap water and mineral oil ($857\ kg\ m^{-3}$, $13.6\ mPa\ s$, $0.029\ N\ m^{-1}$) as test fluids. The asymmetric dimple parameter r_V^* was taken as 0.007 as suggested by Pereyra et al (2013). The initial drop diameter was assumed to be 250 μm and a hindered settling parameter C_h of 0.2 produced reasonable results. Oil-in-water dispersions with an oil fraction of 0.40 were studied at three different mixture velocities: $u_M = 0.06\ m\ s^{-1}$, $0.09\ m\ s^{-1}$, and $0.13\ m\ s^{-1}$. The results are presented in Fig. 6.

The model predicts the location of the *settling curve* y_C with reasonable accuracy when a hindered settling parameter of 0.2 is used. This suggests that the initial model by Pilhofer and Mewes (1979) which was developed for batch systems, overestimates the settling rate of separating dispersed pipe flows even at low mixture velocities. Comparison of the results in Figs. 4 and 5 with the results in Fig. 6 suggest a possible correlation between the mixture velocity and the hindered settling parameter. However, further studies are required to establish a relationship. The results also suggest that the current model can be used without accurate knowledge of the initial drop size, as long as there is enough data to fit C_h (i.e. measurements of y_C or y_P).

The characteristic layers evolve in a similar manner in the three cases, but there is a clear positive correlation between the mixture velocity and the separation length. Initially, the dispersions consist of settling and dense-packed layers. The dense-packed layers deplete first, while the settling layers persist up to the point of complete separation. The depletion of the dense-packed layer even at low mixture velocities suggests that this flow-pattern transition may be common in several setups in industry and highlights its significance.

Finally, the applicability of the model to water-in-oil dispersions was investigated for three hypothetical cases. The average drop diameters and the initial thicknesses of the continuous phase, the dispersed phase, and the dense-packed layer were taken to be the same as the corresponding oil-in-water cases studied above. Due to the lack of experimental data, the dimensionless asymmetry coefficient, r_V^*, was assumed to be the same as in the oil-in-water cases. Although this could be the case and such fluid combinations have been identified in the past, Henschke et al. (2002) argues that it cannot be concluded that this is always so, hence the results need to be treated with caution.

The results presented in Fig. 7 show the predicted length required for

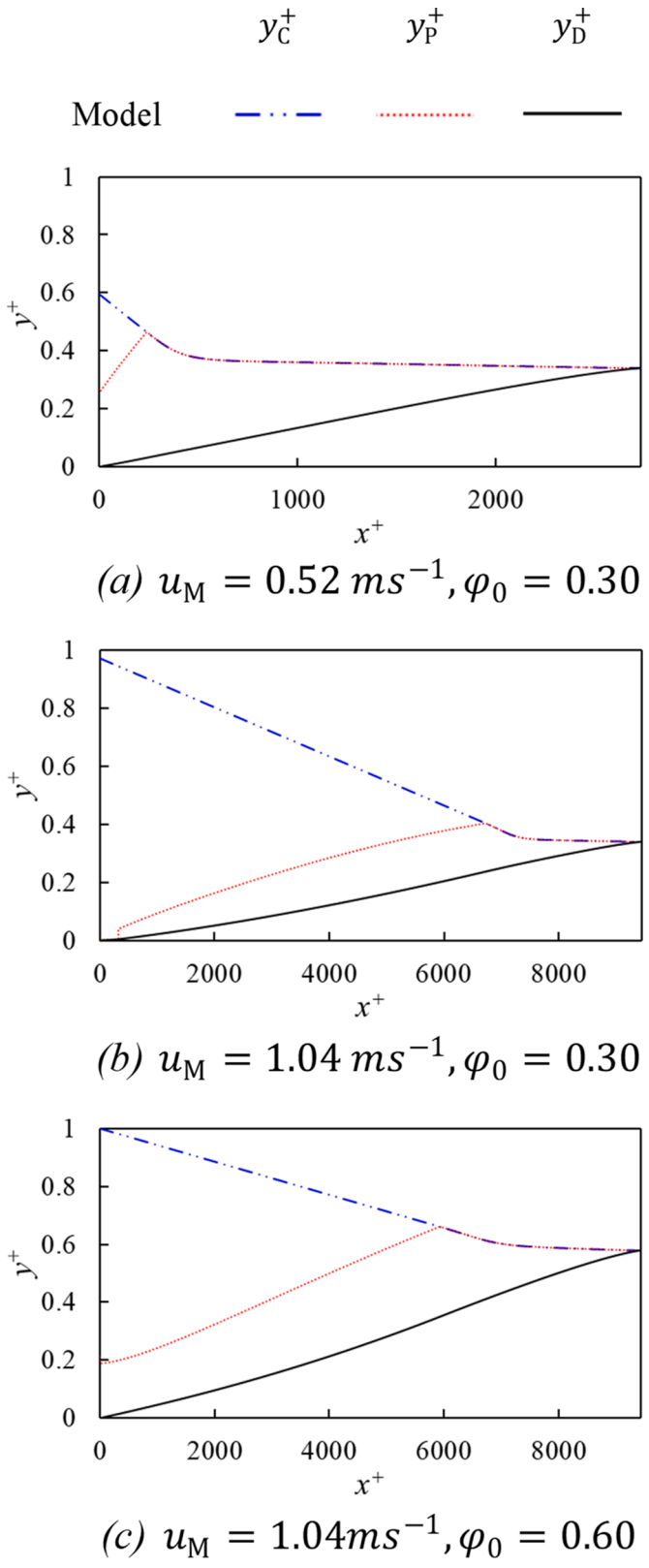

Fig. 7. Prediction of the flow profiles for water-in-oil dispersions.

separation to be significantly larger for water-in-oil dispersions than for oil-in-water ones. This is due to the lower coalescence rates predicted for the water-in-oil cases. In the case shown in Fig. 7(a), the settling layer depletes at a similar axial length as the corresponding oil-in-water case (cf. Fig. 4(a)), however the lower coalescence rates cause the dense-packed layer to persist for longer before complete separation occurs. Fig. 7(b) shows the formation of a dense-packed layer from an almost fully dispersed inlet, in contrast to the corresponding oil-in-water case (cf. Fig. 5(b)) where the dense-packed layer never forms. Finally, in the case in Fig. 7(c) the dense-packed layer initially grows in thickness and persists up to the point of complete separation. This is again contrary to the corresponding oil-in-water case (cf. Fig. 5(d)) where the dense-packed layer depletes first and the settling layer remains until separation occurs.

5. Conclusions

In this work, a methodology for the prediction of the separation of dispersed liquid-liquid flows in horizontal pipes was presented, which is based on the physical mechanisms of drop settling, drop-interface coalescence, and drop-drop coalescence and uses two fitted parameters, C_h and r_V^*. The proposed model predicted the evolution of the pure water layer, the settling layer, the dense-packed zone, and the pure oil layer up to the point of complete separation for both oil-in-water and water-in-oil systems. The predicted characteristic layer thicknesses for initial oil-in-water dispersions demonstrated little deviation from the available experimental measurements. The increase in drop size due to drop-drop coalescence was also well captured. It was shown that depending on the inlet and flow conditions, the separation can be either coalescence-controlled or settling-controlled, and different flow patterns and flow pattern transitions can arise. It was also found that the drop size has a major effect on the rate of settling, hence smaller drop sizes are more likely to lead to settling-controlled separation. Nevertheless, in this work we have shown that accurate drop-size measurements of the initial dispersion are not required. The hindered settling parameter can compensate for any inaccuracies in the drop size and produce reasonable results for thickness of the various layers. A relationship between mixture velocity and the hindered settling parameter is likely, but further studies are required to establish it. The continuous phase affects the rate of coalescence. Lower rates of coalescence were predicted for the oil-continuous systems, hence in those cases the dense-packed layer was more likely to form and persist up to the point of complete separation.

The model presented here can be used to swiftly predict the evolution of liquid-liquid dispersions for industrial applications. While the findings are encouraging, further experimental data would help validate the model at different pipe lengths and specifically, data closer to the point of complete separation. In addition, allowing for different drop sizes could increase the accuracy of the model.

CRediT authorship contribution statement

Nikola Evripidou: Conceptualization, Methodology, Software, Writing – original draft. **Carlos Avila:** Supervision. **Panagiota Angeli:** Supervision, Writing – review & editing, Funding acquisition.

Declaration of Competing Interest

The authors declare that they have no known competing financial interests or personal relationships that could have appeared to influence the work reported in this paper.

Acknowledgements

Nikola Evripidou is grateful to Chevron Corporation and to University College London for the IMPACT studentship. The authors would also like to thank Dr Victor Voulgaropoulos for providing the experimental data.

References

Angeli, P, Hewitt, GF, 2000. Flow structure in horizontal oil–water flow. In: Int. J. Multiphase Flow 26.7, 1117–1140.

Barnea, E, Mizrahi, J, 1975. Separation mechanism of liquid/liquid dispersions in a deep-layer gravity settler: Part I-the structure of the dispersion band. Trans. lnstn chem. Engrs 53, 61–69.

Conan, C, Masbernat, O, Décarre, S, Liné, A, 2007. Local hydrodynamics in a dispersed-stratified liquid–liquid pipe flow. AIChE J. 53 (11), 2754–2768.

Coulaloglou, CA, Tavlarides, LL, 1977. Description of interaction processes in agitated liquid-liquid dispersions. Chem. Eng. Sci. 32 (11), 1289–1297.

Danielson, TJ, 2012. Transient multiphase flow: past, present, and future with flow assurance perspective. Energy & Fuels 26 (7), 4137–4144.

Dörr, A, Sadiki, A, Mehdizadeh, A, 2013. A discrete model for the apparent viscosity of polydisperse suspensions including maximum packing fraction. J.Rheol. 57 (3), 743–765.

El-Batsh, HM, Doheim, MA, Hassan, AF, 2012. On the application of mixture model for two-phase flow induced corrosion in a complex pipeline configuration. Appl. Math. Modell. 36 (11), 5686–5699.

Elseth, G, 2001. An experimental study of oil/water flow in horizontal pipes. PhD Diss. Telemark University College.

Evripidou, N, Voulgaropoulos, V, Angeli, P, 2019. Simplified mechanistic model for the separation of dispersed oil-water horizontal pipe flows. BHR 19th International Conference on Multiphase Production Technology. BHR Group.

Farr, RS, Groot, RD, 2009. Close packing density of polydispersehard spheres. The J. Chem. Phys. 131 (24), 244104.

Hartland, S, Jeelani, SAK, 1988. Prediction of sedimentation and coalescence profiles in a decaying batch dispersion. Chemi. Eng. Sci. 43 (9), 2421–2429.

Henschke, M, Schlieper, LH, Pfennig, A, 2002. Determination of a coalescence parameter from batch-settling experiments. Chem. Eng. J. 85 (2-3), 369–378.

Ishii, M, Zuber, N, 1979. Drag coefficient and relative velocity in bubbly, droplet or particulate flows. AIChE J. 25 (5), 843–855.

Jeelani, SAK, Hartland, S, 1994. Effect of interfacial mobility on thin film drainage. J. Colloid and Interface Sci. 164 (2), 296–308.

Jeelani, SAK, Hartland, S, 1998. Effect of dispersion properties on the separation of batch liquid- liquid dispersions. Ind. Eng. Chem. Res. 37 (2), 547–554.

Lovick, J, Angeli, P, 2004. Droplet size and velocity profiles in liquid–liquid horizontal flows. Chem. Eng. Sci. 59 (15), 3105–3115.

Oddie, G, Pearson, JRA, 2004. Flow-rate measurement in two-phase flow. Annu. Rev. Fluid Mech. 36, 149–172.

Othman, H, Dabirian, R, Gavrielatos, I, Mohan, R, Shoham, O, 2018. Validation and improvement of the horizontal pipe separator model. SPE Western Regional Meeting. Society of Petroleum Engineers.

Pérez, CA, 2005. Horizontal pipe separator (HPS©) experiments and modeling. PhD Diss. University of Tulsa.

Pereyra, E, Mohan, R, Shoham, O (2013). "A simplified mechanistic model for an oil/water horizontal pipe separator". In: Oil and Gas Facilities 2.03, pp. 40–46.

Pilehvari, A, Saadevandi, B, Halvaci, M, Clark, PE, 1988. Oil/water emulsions for pipeline transport of viscous crude oils. SPE Annual Technical Conference and Exhibition. OnePetro.

Pilhofer, T, Mewes, D, 1979. Siebboden-Extraktionskolonnen: Vorausberechnung unpulsierter Kolonnen. Verlag Chemie.

Pouraria, H, Kwan Seo, J, Kee Paik, J, 2016. CFD simulation of the effect of different oils on water wetting and internal corrosion of oil pipelines. International Conference on Offshore Mechanics and Arctic Engineering. Vol. 49965. American Society of Mechanical Engineers. V005T04A023.

Rodriguez, OMH, Oliemans, RVA, 2006. Experimental study on oil–water flow in horizontal and slightly inclined pipes. Int. J. Multiphase Flow 32 (3), 323–343.

Ryon D, A, Daley L, F, Lowrie S, R, 1960. Design and scale-up of mix-settlers for the Dapex Solvent Extraction Process, Report No. ORNL-2951. Oak Ridge National Laboratory, Tennessee, U.S.A.

Simmons, MJH, Azzopardi, BJ, 2001. Drop size distributions in dispersed liquid–liquid pipe flow. Int. J. Multiphase Flow 27 (5), 843–859.

Skjefstad, H, Stanko, M, 2019. Experimental performance evaluation and design optimization of a horizontal multi-pipe separator for subsea oil-water bulk separation. J. Petroleum Sci. Eng. 176, 203–219.

Trallero, JL, Sarica, C, Brill, JP (1997). "A study of oil-water flow patterns in horizontal pipes". In: SPE Production & Facilities 12.03, pp. 165–172.

Voulgaropoulos, V, Zhai, L, Ioannou, C, Angeli, P, 2016. Evolution of unstable liquid-liquid dispersions in horizontal pipes. 10th North American Conference on Multiphase Technology. BHR Group.

Voulgaropoulos, V, 2017. Dynamics of spatially evolving dispersed flows. PhD Diss. University College London.

Voulgaropoulos, V, Angeli, P, 2017. Optical measurements in evolving dispersed pipe flows. Experiments in Fluids 58 (12), 170.

Voulgaropoulos, V, Jamshidi, R, Jamshidi, R, Angeli, P, 2019. Experimental and numerical studies on the flow characteristics and separation properties of dispersed liquid-liquid flows. Phys. Fluids 31 (7), 073304.

Walvekar, RG, Choong, TSY, Hussain, SA, Khalid, M, Chuah, TG, 2009. Numerical study of dispersed oil–water turbulent flow in horizontal tube. J. Petroleum Sci. Eng. 65 (3-4), 123–128.

Wang, ZM, Zhang, J, 2016. Corrosion of multiphase flow pipelines: the impact of crude oil. Corrosion Rev. 34 (1-2), 17–40.

Zhong, X, Wu, Y, Li, S, Wei, P, 2013. Investigation of pipe separation technology in the oilfield. Advanced Materials Research. Vol. 616. Trans Tech Publ, pp. 833–836. .a.